Colloids and Surfaces A 564 (2019) 39–50

Contents lists available at ScienceDirect

Colloids and Surfaces A

journal homepage: www.elsevier.com/locate/colsurfa

Physicochemical characterization of albumin immobilized on different TiO_2 surfaces for use in implant materials

Erika S. Bronze-Uhle[a,*], Leonardo F.G. Dias[a], Luciana D. Trino[a], Adriana A. Matos[b], Rodrigo C. de Oliveira[b], Paulo N. Lisboa-Filho[a]

[a] UNESP São Paulo State University School of Sciences, Department of Physics, Bauru, São Paulo, Brazil
[b] Department of Biological Sciences, Bauru School of Dentistry, University of São Paulo, Bauru, São Paulo, Brazil

GRAPHICAL ABSTRACT

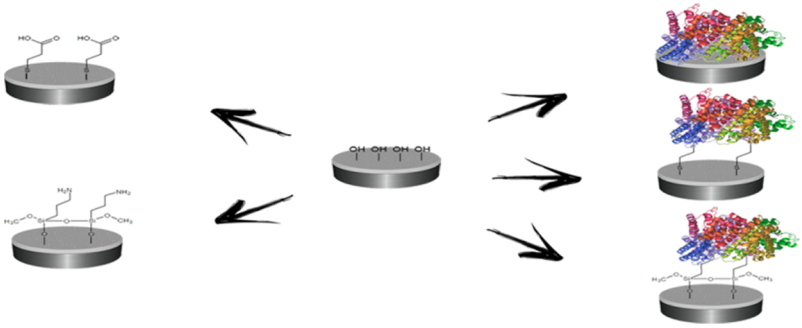

ARTICLE INFO

Keywords:
Titanium
Titanium dioxide
3- Mercaptopropionic acid (MPA)
3-Aminopropyltrimethoxysilane (APTMS)
Albumin adsorption and bone implant materials

ABSTRACT

Osseointegration process may be defined as the structural and functional connection between living bone and the surface of an implant, promoting adequate cell adhesion, proliferation, and differentiation. One strategy to increase the biocompatibility and consequently generate greater osteogenesis is to modify the surfaces of implants to alter the process of the bone tissue repair. Surface modifications in titanium implants were proposed using organic bifunctional spacers (3-mercaptopropionic acid, MPA, and 3-aminopropyltrimethoxysilane, APTMS) or direct albumin (BSA) immobilization. Chemical immobilization of BSA, either physically or covalently, on TiO_2 substrates showed similar surface chemistry without altering long-term cellular interaction. Furthermore, TiO_2-APTMS substrate with $-NH_2$ groups on the surface more efficiently interacts with components of the extracellular matrix, presenting high cell viability at 48 h and better viability and mineralization results.

1. Introduction

Implants currently used in dentistry or orthopedic surgery are mostly produced from metallic materials, with pure titanium and/or its derivatives alloys commonly employed. Titanium is attractive due to its physical and chemical properties, such as corrosion resistance, excellent mechanical properties, and superior biocompatibility compared to other alloys [1–4]. However, serious problems associated with biocompatibility and frequent incidence of infections still exist, which are the primary causes of implant failures and rejections [5,6]. In addition, metallic titanium has hydrophobic surface properties, which caused poor interface with biological cells and may prohibit cell adhesion

* Corresponding author.
E-mail address: eriuhle@fc.unesp.br (E.S. Bronze-Uhle).

https://doi.org/10.1016/j.colsurfa.2018.12.028
Received 12 September 2018; Received in revised form 28 November 2018; Accepted 13 December 2018
Available online 14 December 2018
0927-7757/ © 2018 Elsevier B.V. All rights reserved.

[7,8].

The osseointegration process is a prerequisite for the success of an implant, so the implant surfaces should promote adequate cell adhesion, proliferation, and differentiation, to generate the formation of healthy bone at the osseointegration interface. One of the strategies to increase the biocompatibility and generate greater osteogenesis to avoid infections is by modifying the surfaces of these implants to alter the bone tissue repair process [9–13]. The hydrophilic property of the substrate is important for more effective interaction with the titanium surface, because the relative wettability and hydrophilicity of the surface are determinant factors for the degree of adhesion and migration cells [14].

Surfaces modifications in titanium may involve topographical and compositional changes, at the micro and nanoscale, to simulate the characteristics of natural bone in the osseointegration process [15–17]. These modifications alter the physical properties, such as morphological, chemical, and wettability of the surface, modifying the final biological properties [18–21].

Studies increasingly emphasize that a substrate with hydrophilic properties has more effective cellular interaction [4]. Vilardell et al. [21] and Mekayarajjananonthet [22] reported a number of studies correlating surface factors such as rugosity, surface energy, contact angle values, and cell adhesion with biomaterial surfaces [23].

The excellent biocompatibility of Ti is due to the surface oxide film spontaneously formed on its surface with a few nanometer titanium dioxide (TiO_2) thick Ti. However the extremely thin layer (5–6 nm) is not able to prevent long term corrosion and leads to implant failure. Werner et al. [24] reported that the thicker crystalline and homogeneous layer of TiO_2 (100 nm) on the titanium surface significantly increases the long-term bio-corrosion of titanium resistance and provides better adhesion and proliferation of osteoblasts. In addition, the native oxide layer was generally less hemocompatible compared to a thicker and more homogeneous layer of TiO_2 [24–27]. Therefore, the TiO_2 deposition in the nanometric and crystalline phase with controlled surface chemistry and hydrophilicity is extremely important in the bone integration process [27–29]. In addition, biomedical research has focused on modified TiO_2 surfaces that can optimize the early stages of osseointegration, improving bone bonding between bone and implant [32,33].

Titanium surface modification with TiO_2 nanometric films can be obtained by different deposition methods, among them, chemical spin coating method. This method changes not only the titanium topography or morphology, but also other surface characteristics, such as crystallinity, chemical composition, wettability, and adsorption capacity [29–31].

Titanium dioxide layers are chemically terminated mainly by hydroxyl (-OH) groups, under ambient conditions, which can dissociate into solution, generating positive, negative, or neutral charges, depending on the pH of the solution. This surface and the charges formed by the dissociation presents an important role in the interaction with polymers, proteins, and immobilization of organic molecules [34,35]. The interaction with the TiO_2 substrate can be covalent or non-covalent. The process modifies the surface energy of the material, macro and micro morphology, because it alters the functional groups and their mobility on the substrate surface to be implanted. These physical chemical alterations change the hydrophilicity and electrostatic properties of the surface responsible for cell interaction, adhesion, and proliferation of osteoblasts [36].

A promising alternative for surface modification is the immobilization of bioactive molecules, such as proteins and peptides, on the surface of the metal material [35,37,38]. The adsorption of proteins on the TiO_2 surface occurs through physical adsorption of the -OH groups on the surface, by electrostatic, hydrophobic, hydrogen bonding, and van der Waals interactions [39–42]. The protein and/or peptide layer under the surface is unstable and flexible, since this adsorption is preferentially given by reversible electrostatic interactions [43–45]. Therefore, proteins can adopt many conformations under the surface of the substrate, because they interact with the TiO_2 surface at many sites [46,47]. The size, charge, and surface composition of the proteins may lead to a complex adsorption process with various intermediates, conformations, and/or orientations on the TiO_2 surface [48], promoting dynamic protein adsorption/desorption processes. Thus, immediately after implantation and contact with biological fluids and components of the extracellular matrix, the protein layer can be removed into the medium [35].

These biomolecules have great potential to adsorb into almost all types of interface, due to the presence of amino acids in their protein chains, which are on their surface hydrophobic regions, uncharged polar and charged polar regions. Thus, the interactions may be due to hydrophilicity, hydrophobicity, ionic interactions, or by the formation of covalent bonds with a specific functional group of the molecule [43,49,50]. Systematic studies of biological responses to artificial materials require surfaces with well-controlled properties, and a variety of procedures have been applied to optimize the orientation and conformation of immobilized proteins on implant surfaces, such as fixation through load-driven orientation [51–53], adsorption through hydrophobic interactions [54–56], and covalent interactions by bioactive bifunctional compounds (ligand molecules) [57–59]. Frequently, binding molecules act as spacers, which provide greater steric freedom to the protein, allowing more specific activity [35].

The presence of hydroxyl groups (-OH) on the TiO_2 surface allows the occurrence of condensation reactions, through the formation of covalent bonds with bifunctional bioactive organic binders, generating self-assembled monolayers (SAMs) on the oxide surface [35,59,60].

These organic linkers have two functional groups. One of the functional groups interacts with the hydroxyls of the TiO_2 substrate, while the other organic group of the ligand interacts with the protein sites, to modify the chemical interface between the titania substrate and the biological environment [57,60–63]. The introduction of carboxy acid, esters, amine, sulfonated and/or thiol organic groups on the TiO_2 surface can be effective ways to conjugate various biomolecules by these functional groups [64]. The formation of SAMs alters many factors relevant to cell-implant interaction, including the surface energy of the material, macro and micro-morphology. These factors modify the electrostatic property of the surface responsible for the interaction and consequently cell adhesion and proliferation [61,65,66].

Protein covalent immobilization can substantially improve the stability of the resulting coatings through its irreversible manner compared to the physical adsorption of the protein on the substrate surface. In addition, covalent immobilization also allows better control over substrate surface parameters, such as thickness, binder density, and molecular orientation of the protein [31,35].

The proteins interaction with the implant surface plays an important role in the integration of the implant with the surrounding tissue as well as its biocompatibility and functionality. The adsorption of proteins on the surface of the implant is the first event that occurs after implantation, followed by cell adhesion and proliferation. Which cells will adhere on the surface depends on the type of protein adsorbed on the surface. Therefore, surface modification (functionalization) of the implant surface is very import to control cell and/or protein-surface interactions [13,35].

Numerous serum proteins, including albumin, fibrinogen, and fibronectin, have been studied in relation to their adsorption into the implant surface of materials and subsequent cellular responses [67]. Among them, albumin is a globular transport protein very well characterized and used in adsorption studies due to its abundance in plasma, constituting about 50% of the proteins in plasma. Some studies have shown that, in relation to other metal oxides, albumin has better adhesion with titanium dioxide, which occurs as a function of the oxide surface being positively charged, that is, depending on the surface charge density [68,69].

Self-assembled monolayers of alkanethiols ($HS(CH_2)_nX$ derivatives)

[70] and coupling agents derived from silane ($(CH_3\text{-}O)_3Si(CH_2)$ nX, where X is another functional group, are used to bind biomolecules in different materials with hydroxyl groups on their surface [71–73] and are suitable to study correlations between surface properties and biological responses. Therefore, the aim of this study was to evaluate the influence of surface chemistry involved in albumin immobilization (BSA) directly on the TiO_2 surfaces or by organic spacer linkers. In this study, 3-mercaptopropionic acid (MPA) and 3-aminopropyltrimethoxysilane (APTMS) were used as organic bifunctional spacers on TiO_2 surfaces. As is known, one of the functional groups of MPA (thiol and/or carboxylic acid) and APTMS (amine and/or silane) bind covalently on the TiO_2 surface through hydroxyl groups present on the surface, generating a new chemical interface, with different physicochemical properties. After the TiO_2 deposition, the substrates were immediately functionalized with the different chemical groups (3-mercaptopropionic acid (MPA), 3-aminopropyltrimethoxysilane (APTMS) and bovine serum albumin (BSA)) by immersion method. The interaction of the BSA on the TiO_2 surface and with the respective substrates functionalized with MPA and APTMS were characterized. The objective was to evaluate the effects of chemical, morphology, wettability, surface functional groups, and cell osteoblast adhesion using different BSA interaction on the surface.

2. Materials and methods

2.1. Materials

All materials and reagents were used with analytical grade and purchased from Sigma-Aldrich, as commercially received. Deionized water was used for all aqueous solutions obtained with a Millipore Milli-Q system. Titanium discs were prepared from commercially pure titanium specimens grade 4 (Ti cp4, 12.7 mm in diameter and 3 mm in thickness) from Bior-Acnis (Brazil).

2.2. TiO_2 synthesis solutions

In the present study, TiO_2 solution synthesis was prepared according to the method described by Trino, L.D and Bronze-Uhle, E. S et al. [74].

2.3. Preparation and modification of titanium substrates

The Ti cp4 discs were polished in an Arotec polisher (Aropol-2v model) using sandpapers with 320, 400, 600 and 800 granulometry, for two minutes each.

The substrates were cleaned were cleaned in a series of ultrapure water-isopropyl alcohol and ultrapure water, for ten minutes each in an ultrasonic cleaner, to remove all the sandpapers impurities. To alter the surface chemistry, Ti cp4 discs were etched and hydroxylated in a highly acidic piranha solution mixture of 7:3 (v/v) 98% H_2SO_4 and 30% H_2O_2) for two hours and, subsequently were rinsed in an ultrasonic cleaner with the same procedure as before for immediate oxide deposition [74,75].

Spin coating technique (2000 RPM per 60 s) was used to perform the TiO_2 solution deposition using a Headway Research INC (model PWM32-PS-R720) equipment. For spin process deposition, three drops of TiO_2 solution were added over the metallic surface substrate. After rotation, the substrates were placed in a hot plate at 40 °C for 5 min. The process was repeated three times for each sample. Subsequently, the Ti cp4 substrates coated with TiO_2 were annealed at 850 °C for two hours at a heating rate of 1 °C min^{-1}. The rutile crystalline polymorphic phase was obtained [74].

2.4. Methods of SAM preparation

2.4.1. Surface modification of TiO_2 substrates with organic bifunctional compounds

For SAM TiO_2 preparation, two different bifunctional form molecules were used as organic spacers: 3-mercaptopropionic acid (MPA) and 3- aminopropyltrimetoxysilane (APTMS). The functionalization of samples occurred by the immersion method as described below.

2.4.2. 3-mercaptopropionic acid (MPA)

The 3 mM MPA aqueous solution was prepared adjusting the pH solution to 3 using HCl. The substrates were immersed for 1 h at room temperature of 25 °C. After the immersion period, substrates were washed 3 times with water to remove the molecules physically adsorbed on the surface [76].

2.4.3. 3-aminopropyltrimetoxysilane (APTMS)

The 3 mM APTMS solution was prepared in ethanol. After complete dissolution, the substrates were immersed for 1 h at room temperature of 25 °C. Then, the samples were washed 3 times with ethanol to remove from the surface physically adsorbed molecules [77].

2.4.4. Protein adsorption: albumin functionalization

Bovine serum albumin (BSA) solution was prepared at PBS in a 0.40 mg/mL concentration until completed dissolution. The TiO_2 and TiO_2 modified surfaces were immersed in a protein solution for 6 h at room temperature (25 °C). After protein adsorption, substrates were removed from BSA solution and rinsed with PBS (2x) and deionized water (2x) to remove unbounded proteins and salt PBS residues. Subsequently, the substrates were dried, and surface properties were analyzed and characterized [78].

2.5. Surface characterization

2.5.1. XRD

The crystal structure of the TiO_2 films was analyzed by X-ray diffraction (XRD, D/MAX-2100/PC, Rigaku) using CuKα radiation within (k = 1.54056 Å) coupled to a nickel. The samples were scanned from 20° to 45°, with regular step of 0.02° min^{-1} and scan speed of 2° min^{-1}, at 40 kV/20 mA. The XRD pattern of the samples were compared with PCPDF 65–3411, 44–1294, and 76–1949 cards for Ti and TiO_2, respectively.

2.5.2. XPS

The surface composition and chemistry were analyzed using X-ray photoelectron spectroscopy (XPS, K-Alpha -Thermo Scientific) equipped with an Al Kα micro-focused monochromator with variable spot size (30–400 μm in 5 μm steps) and energy range 100–4000 eV. Survey scans were completed on each region, followed by high resolution scans. Scans were aligned to the binding energy of the Ti 2p3/2 peak at 458.8 eV. Curve fitting was performed using the CasaXPS software. Peak identification was done to obtain a consistent fit for all the potentials investigated. [79] The functional groups on the surfaces were confirmed by the appearance of characteristic peaks corresponding to the specific covalent bond formation and/or attachment molecule conformation.

2.5.3. Contact angle and surface energy

Surface wettability of the substrates was determined by the contact angle and energy surface with a goniometer (Ramé-Hart 100-00, Succassuna, NJ), using the sessile drop technique. Deionized water (polar substance) and diiodomethane (non-polar substance) were used as probe liquid. At least three droplets were deposited on different positions of the samples and contact angle was measured at each side of the drop. Measurements were performed in triplicate, at room temperature, and under controlled humidity environment. The contact

angle and surface energy were evaluated by DROPimage software based on the Young-Laplace equation describing the drop profile of sessile drops [80].

2.5.4. AFM

Modified surface structure and morphology were analyzed by atomic force microscopy (AFM, Park System XE7, Santa Clara, CA, USA). Surface topography images was conducted in non-contact mode and collected using a silicon cantilever (PPP-NCHR, Park Systems Inc.) having a constant force of 42.0 N/m and resonance frequency of 330 Hz. The substrates were scanned in air under room temperature conditions. The images were taken using a scan rate in the range of 0.7 Hz, a peak force set point of 9.0 V, and a scan size performed over a 4.0 μm × 4.0 μm.

The average roughness represented by the root mean square (rms) roughness of the surface was calculated based on a standard formula integrated in the imaging software.

2.6. In vitro biocompatibility

2.6.1. Cell culture

For the cell culture, mouse preosteoblast MC3T3-E1 (subclone 14) cells (ATCC-American Type Culture Collection) were cultured at 37 °C in α-MEM (Minimum Essential Medium α - Gibco, Carlsbad, CA, USA) supplemented with 10% FBS (Fetal Bovine Serum, Gibco), 1% of 10.000 U penicillin-10 mg/mL streptomycin (Sigma-Aldrich) under humidified atmosphere with 5% CO_2. After reaching the subconfluency, the cells were detached using the enzyme trypsin (0.25% trypsin, 1 mM EDTA - Sigma-Aldrich), for 5 min in the CO_2 incubator at 37 °C. The enzyme was inactivated with α-MEM containing 10% FBS. Cells suspensions were centrifuged at 1200 rpm, 5 min at 4 °C. The supernatant was discarded, and the cell pellet were diluted in a new α-MEM 10% FBS medium. To reduce the contamination risk, titanium samples (Ticp4, TiO_2, TiO_2-MPA, TiO_2-MPA-BSA, TiO_2-APTMS, TiO_2-APTMS-BSA and TiO_2-BSA) were maintained for 30 min in ultraviolet light prior to cell paltiing [81].

2.6.2. MTT reduction assay

To determine the cell viability, the MTT (3- (4,5-dimethylthiazol-2-yl) -2,5-diphenyltetrazolium bromide) reduction method assay was performed based on the ability of mitochondrial enzymes. In this procedure, viable cells express higher metabolic activity, by converting the yellow water-soluble tetrazolium salt MTT into a purple-colored formazan product with a maximum absorbance near 550 nm. Thus the formazan production is an indirect indication of cell viability obtained through corresponding colorimetric absorbance proportional to the number of viable cells. For the MTT assay, 2×10^4 cells in 0.050 mL medium (αMEM + 10% FBS + 1% antibiotic) were carefully added on the surface of each substrate to prevent cell adhesion. After 4 h of incubation, at 37 °C in a humidified atmosphere with 5% CO_2, 1.0 ml of medium was then carefully added into each well. MTT assay was performed in triplicate after 48 and 72 h of cell culture incubation. In each experimental period, the wells were washed with phosphate buffered saline solution (PBS 1X) and then the substrates were incubated in a sterile MTT solution (500 μL, 0.5 mg/mL) in a humidified atmosphere containing 5% CO2 at 37 °C for 4 h in the dark. The solution was removed and the MTT formazan was dissolved with 300 μL of dimethyl sulfoxide (DMSO) for 30 min in the dark at room temperature. The extracted contents (250 μL) were transferred to another 96-well plate to allow reading by absorbance at 550 nm (Synergy ™ Mx Monochromator-Based Multi-Mode Microplate Reader, BioTek Instruments Inc.) [82,83].

2.6.3. Calcium deposition assay

Quantification of mineralized calcium deposited in the extracellular matrix were performed by alizarin red staining (Sigma-Aldrich). For this assay, the cells (0.050 mL of medium containing 5×10^4 cells/well) cultured as described above, were seeded on the surface of titanium substrates derivatives. After 4 h of incubation, at 37 °C in a humidified atmosphere with 5% CO_2, 1.00 mL of medium was added on the each well plate. The cells were cultured on the 3 replicates, on plastic and differently Ti surfaces, for a period of 14 days. At each predetermined time point, the cell-seeded samples were washed three times with PBS and then fixed in 70% ethanol (0.70 mL) for 1 h at 4 °C and washed PBS again. All of the samples were stained using 0.70 mL of alizarin red in ultrapure water for 10 min at room temperature. The staining solution was removed and the cells were washed three times with ultrapure water and images were taken. A quantification method was obtained by addition of 280 μL of 10% (v/v) acetic acid solution to each well containing the substrate previously stained with alizarin red. The plate was shaking at room temperature for 30 min. After solubilization, 100 μL of the extracted stain, from each substrate, were transferred to eppendorf tubes and then 40 μL NH_4OH 10% was added to neutralize it. The colored supernatant were read in a 96-well plate with a spectrophotometer (Synergy ™ Mx Monochromator-Based Multi-Mode Microplate Reader, BioTek Instruments Inc.) in wavelength of 405 nm [84].

2.6.4. Statistical analysis

Statistical analysis of the cell assays were performed in the Graph Pad Prism 5 software (Graphpad Prism, GraphPad Software Inc., San Diego, CA, USA) by selecting the one-way ANOVA statistical test complemented by the Tukey test, with the level of statistical significance set at $p < 0.05$.

3. Results and discussion

The nanoscale modification of titanium surfaces can alter the physical properties of the surface, modifying the cellular interaction and may facilitate and allow bone formation in materials for medical and dental implants. As already mentioned, the deposition of thin TiO_2 films on the surface and the chemical manipulation of this surface, tends to improve osteoblast adhesion and proliferation properties, by altering the physical and chemical properties at the implant-cell interface.

Initially, thin films of TiO_2 were deposited and characterized on a titanium surface, as reported by Luciana et al. [74] According to the procedure, the TiO_2 films exhibit the XRD pattern for rutile and the presence of strong peak centered at a 27.7° relative of (110) plane, two low peaks can be observed at 25° and 40° relative to anatase, however, the thin film is majority composed of rutile. According to the same study, the particle size is around 75 (± 6.4) nm.

Scanning electron microscopy (SEM) demonstrates that the TiO_2 films have a particle size of about 75 (± 6.4) nm and a thickness of approximately 500 nm [74]. After characterized by XRD and SEM, the TiO_2 substrates were immediately functionalized with the different chemical groups (3-mercaptopropionic acid (MPA), 3-aminopropyltrimetoxysilane (APTMS), and bovine serum albumin (BSA)) to evaluate to evaluate the chemical, physical, and morphological influence of BSA binding on the TiO_2 substrate with or without the presence of bifunctional organic spacer.

The surface chemical composition of the substrates TiO_2, TiO_2-MPA, TiO_2-MPA-BSA, TiO_2-APTMS, TiO_2-APTMS-BSA, and TiO_2-BSA were observed through X-ray photoelectron spectroscopy (XPS). XPS was used to examine the adsorption of the MPA, APTMS bifunctional organic compounds, and the BSA on the TiO_2 surfaces. Fig. 1 shows the survey spectra of the analyzed substrates.

The XPS results show an increase in the intensity of C 1 s (~285 eV) for all functionalized substrates, which indicates the success of the surface modifications. TiO_2 substrate had C1 s peak indicating possible atmospheric contamination. Ti 2p (~454 eV) were observed all the substrates referring to pristine TiO_2. The presence of O 1 s (~530 eV) signal was observed in all the substrates referring to pristine TiO_2 or a

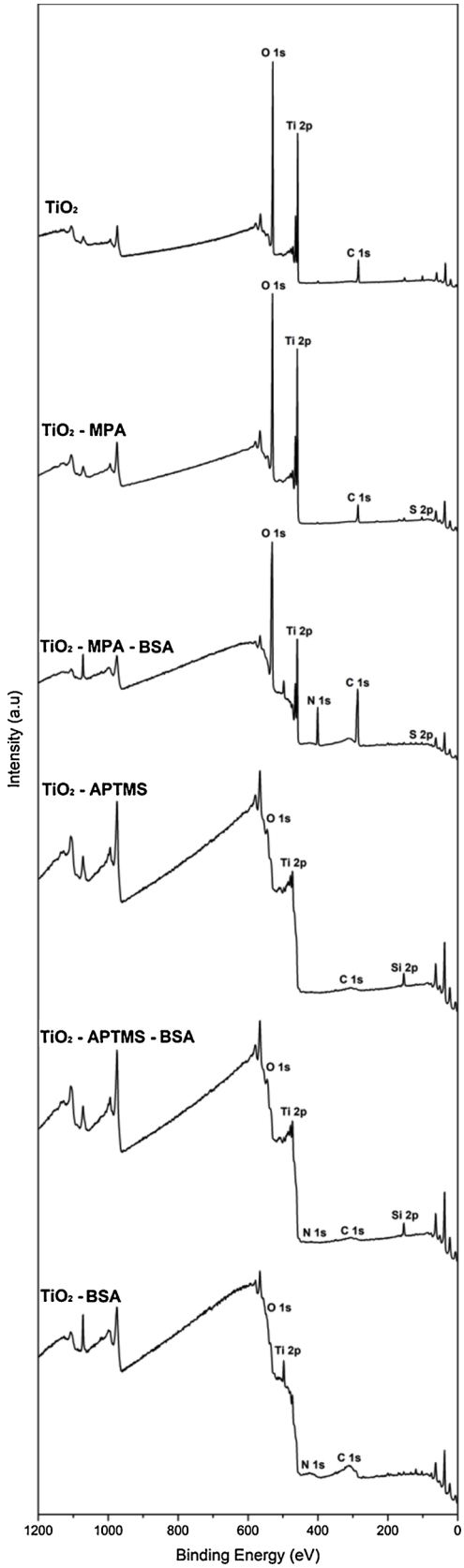

Fig. 1. XPS survey spectrum for the analyzed substrates of TiO_2.

biofunctional group. The presence of S 2p (~ 163 eV) signal for TiO_2-MPA and TiO_2-MPA-BSA confirms the success of thiol functionalization. In the substrates containing APTMS, the presence of signals referring to N 1 s (~ 401 eV) and Si 2p (~ 103 eV), as well as in substrates containing albumin, confirms the surface modification with these biofunctional groups [17,74,76].

3.1. XPS analysis of MPA and APTMS on TiO_2 surface substrate

More chemical information related to the type of bond between the compounds on the TiO_2 surface and which free organic groups on the surface of the TiO_2 substrates were obtained by high resolution XPS scanning. The thiol, carboxylic acid, amino, silane, and hydroxyl organic groups were evaluated, through high resolution spectra for each respective group. The spectra were deconvoluted into different components by a fitting procedure.

The Ti 2p and O 1 s high-resolution XPS spectrum of the TiO_2 surface were taken and corroborate with previously obtained and published XPS signals [17,74]. The 2p3/2 peaks of Ti and TiO_2 are known to be at 453.8 eV and 458.8 eV, respectively. The energy difference between spin orbit peaks Ti $2p^1/_2$ and Ti $2p^3/_2$ is 5.7 eV, which is consistent to Ti^{4+} in TiO_2 bond. By O 1 s high resolution spectrum, two contributions were obtained consistent with Ti-O in TiO_2 and –OH groups on the surface [74].

Analyzing the high-resolution C 1 s, O 1 s, and S 2p spectra of MPA (Fig. 2) on the TiO_2 surface, it is possible to understand a preferential binding mode on both substrates. The deconvolution of C1 s high-resolution spectrum for TiO_2-MPA shows that the main peak has three contributions centered at 284.7 eV, 286.3 eV, and 288.6 eV, referring to C—C, C—S, and free COO- or COOH from MPA, respectively. The O 1 s signal presents two contributions at 530.0 eV and 531.6 eV, which corresponds to TiO_2/ Ti—O and S—O/OH bond, respectively. The TiO_2-MPA shows an S 2p peak with three contributions, centered at 159.5 eV, 164.05 eV, and 168.7 eV relative to S—Ti, C—SH (free MPA on the surface), and S—O bonds, respectively [17,85].

The S 2p analysis make it possible to determine the MPA binding mode under the TiO_2 surface. The presence of the S—O (O 1 s-531.6 eV) contribution is an indication that the thiol groups from MPA interact covalently with the hydroxyl groups of the TiO_2 substrate, leaving the free COO-/COOH groups on the surface, confirmed by the C 1 s (288.6 eV) [17,86]. Fig. 3 presents the high-resolution spectra of C1 s, O1 s, N1 s, and Si 2p for functionalized TiO_2 surfaces with APTMS groups.

Typical high-energy-resolution XPS spectra of C 1 s, N 1 s, and Si 2p were obtained after APTMS functionalization. The high-energy resolution spectrum of carbon C 1 s presented three different contributions that are related to different types of carbon-atom bonds at 285.2 eV, 286.7 eV, and 288.6 eV relative to C—C and/or C—H, C—O, and C—Si—O bonds, respectively. The O1 s spectrum can be deconvoluted in two contributions centered at 530.02 eV and 531.8 eV corresponding to TiO_2/Ti—O and Ti—O—Si bonds, respectively, which indicates the adhesion of APTMS molecules by silane groups [17,74,87]. The deconvolution of N1 s high-resolution spectrum for TiO_2-APTMS shows that the main peak has three contributions centered at 398.9 eV, 400.3 eV, and 401.9 eV, referring to Ti-N, free -NH_2, and C—N bond. Contributions at 401.0 eV may be associated with the zwitterionic amine formation, which is connected with the existence of free NH_2 [88–90]. The high energy Si 2p spectrum of silicon resolution has a contribution centered at 102.9 eV for the Si—O bond. The N 1 s and O 1 s high resolution spectra analysis make it possible to confirm that the APTMS molecules bind covalently with the hydroxyls of TiO_2 across the silane groups, leaving the amine groups free on the surface.

3.2. XPS analysis of albumin immobilization on TiO_2 surfaces

The albumin immobilization on the TiO_2, TiO_2-MPA, and TiO_2-APTMS surfaces were evaluated by XPS. Albumin can adsorb directly on a film surface of attractive electrostatic interacting with —OH groups present on the surface film, or through the covalent attachment

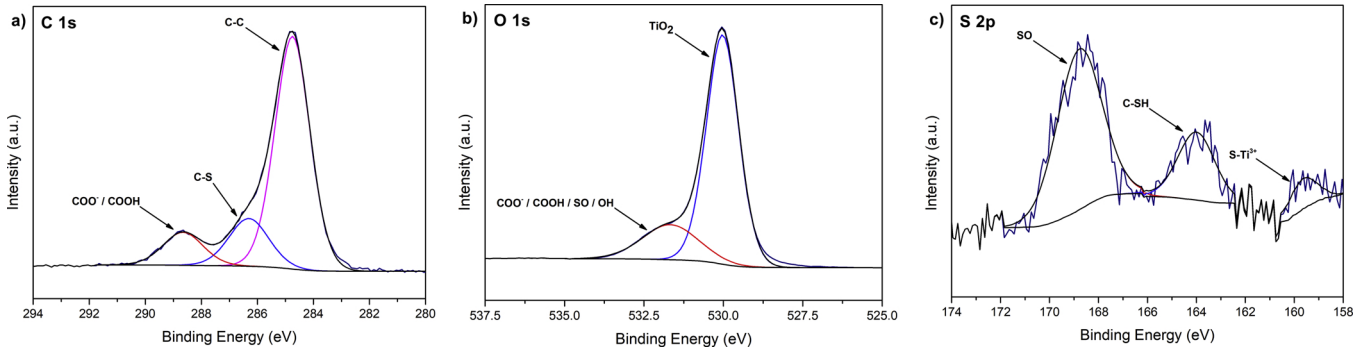

Fig. 2. High-resolution XPS spectra of C 1 s, O 1 s, and S 2p for TiO_2 surfaces functionalized with MPA.

between sites of albumin and functional groups of MPA or APTMS immobilized on the TiO_2 surface. Fig. 4 presents the C 1 s, N 1 s, and O 1 s high-resolution XPS spectra for the TiO_2-BSA, TiO_2-MPA-BSA, and TiO_2-APTMS-BSA.

After protein adsorption, XPS analysis provided more evidence of the presence of proteins on the substrate surface. All the peaks observed on TiO_2-BSA were also observed on TiO_2-MPA-BSA and TiO_2-APTMS. The C1 s deconvolution of TiO_2-BSA spectra presents signals at 285.6 eV, 287 eV, and 288.8 eV referring to C—C/C—H, C—N/C—S, and COO-/COOH/C(O)NH bond, respectively. N 1 s shows contributions at 399.2 eV, 400.6 eV, and 402.2 eV referring to C(O)NH, -NH_2, and C–N bonds, which are typical of albumin on TiO_2 [91,92].

The O 1 s signal after protein adsorption is similar to protein-free, suggesting that most of the signal is attributed to metal oxides (Ti—O) and —OH groups on the surface. The same peak positions are observed on TiO_2-MPA-BSA and TiO_2-APTMS-BSA, indicating the protein adsorption on the surface. Albumin immobilization on the TiO_2-MPA substrate is clearly observed, since C 1 s shows characteristic signs of the presence of albumin on the surface, especially C—N bonds in 286.4 eV, in addition to signals in the N1 s at approximately 402 eV, referring to -NH_2 and C—N.

For the TiO_2-APTMS-BSA substrate, an increase in signal percentage was observed at 400 eV (N1 s) for -NH_2 groups, from 69.2% on TiO_2-APTMS to 83.9% on TiO_2-APTMS BSA. The -$C(O)NH_2$ centered peptide bonds 288.8 eV (C 1 s) increase from 22.2% to 29.6% on the TiO_2-APTMS-BSA substrate. As already explained, the MPA ligand will

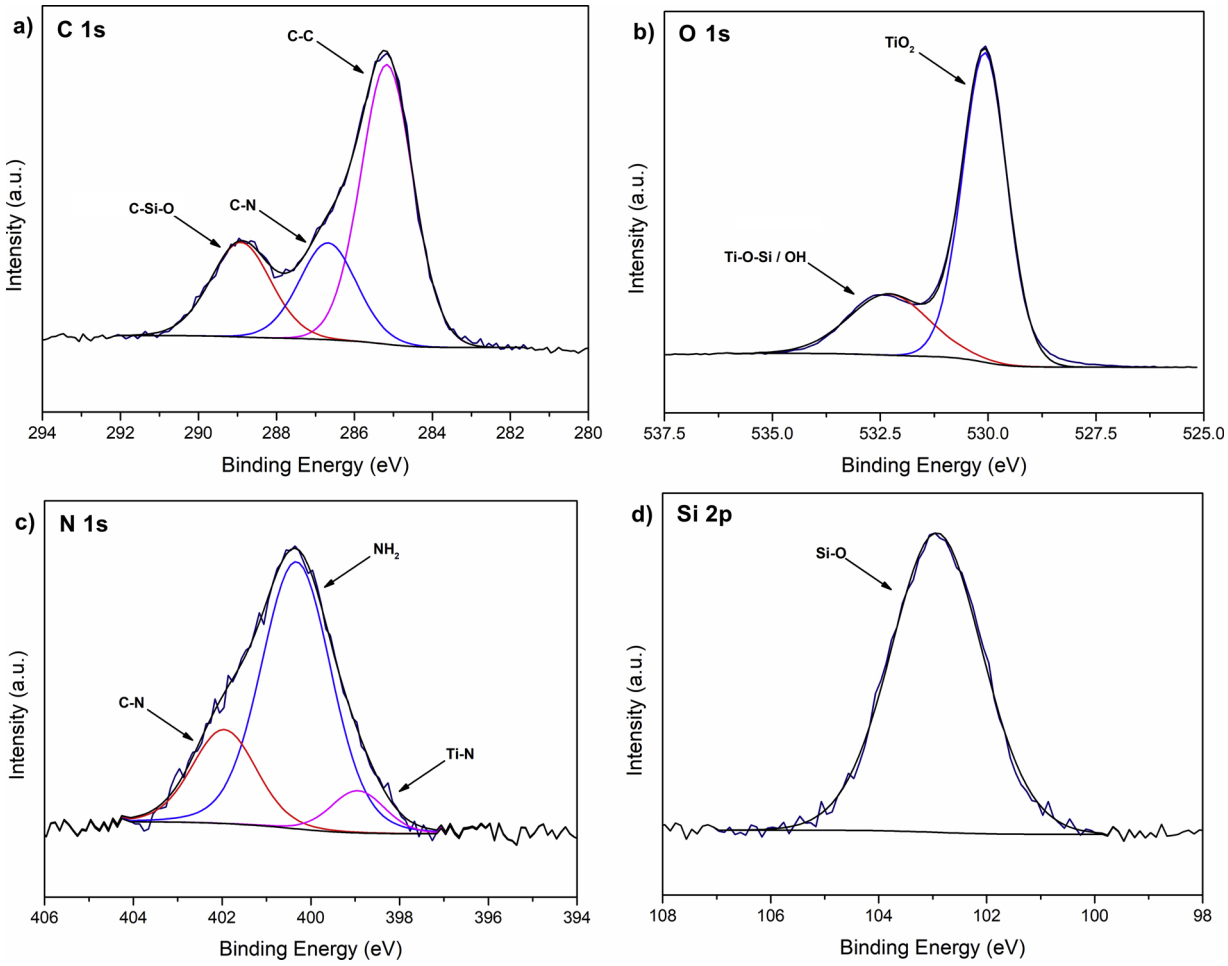

Fig. 3. High-resolution XPS spectra of C 1 s, O 1 s, N 1 s and Si 2p for TiO_2 surfaces functionalized with APTMS.

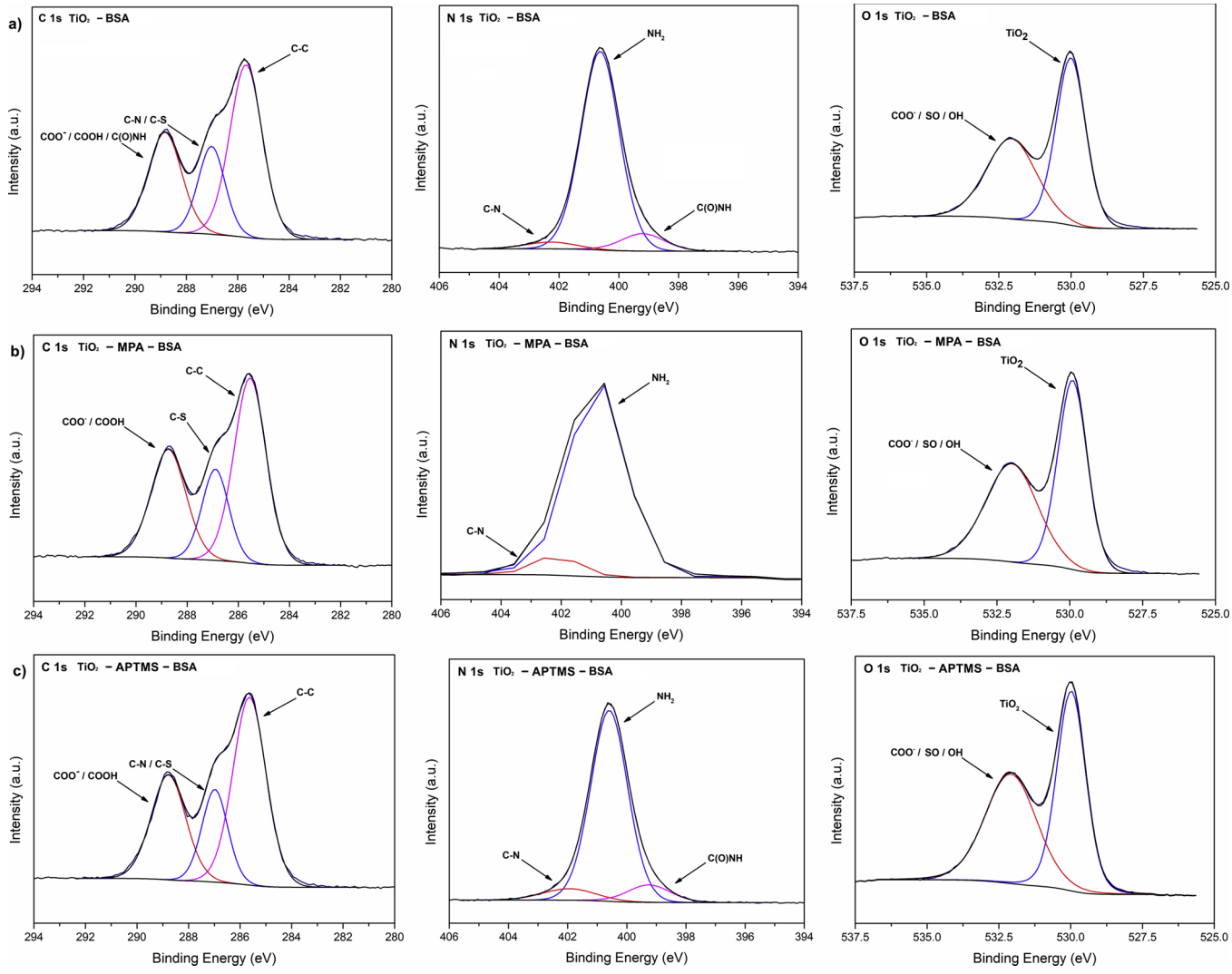

Fig. 4. High-resolution XPS spectra of C 1 s, N 1 s, and O 1 s for TiO_2 surfaces functionalized with BSA.

interact with albumin through free −COOH groups on the surface, whereas APTMS will immobilize the protein through -NH_2 group. Covalent immobilization can not only improve surface uniformity but also provide more precise control of the protein on the surface, such as its fouling, orientation, and availability to attached to cells. The procedures used make the chemical modification in the surface of the substrates clear.

3.3. Surface wettability

The wettability/hydrophilicity and surface energy properties of the functionalized TiO_2 thin films were expected to vary from the pristine TiO_2 films and Ti substrates due to the different functional terminal groups present on their surfaces. It is known that the type of contact is closely related to the moisture and hydrophilicity of the surface, i.e. the lower the contact angle, the greater the wettability and consequently the surface hydrophilicity. The water contact angle (CA) measurements and the energy surface for the analyzed samples are compared in Fig. 5.

Fig. 5a shows the water contact angle (CA) measurements for the analyzed samples. The pristine Ti substrate presented the highest CA value (72°), being the less hydrophilic sample. The presence of TiO_2 thin film presented a mild increase in hydrophilicity, compared to Ti, and had a CA value of 54°. This slight change could be related to the presence of free hydroxyl groups on the TiO_2 surface. After functionalization, an increased wettability was observed for TiO_2-MPA sample to 28°, due to the presence of carboxylic acid terminal groups (−COOH) on the surface. Following the bio-functionalization with albumin, no significant change in wettability was observed for the TiO_2-MPA-BSA sample, which presented a CA of 31°. However, the presence of APTMS bifunctional molecule on the TiO_2 surface provided a more hydrophobic behavior, with a CA of 54° [78]. This could be related to the long carbon chain from the APTMS molecule. After the bio-functionalization with albumin, a decrease to 32° was observed for TiO_2-APTMS-BSA sample. The immobilization of the protein increased the wettability due to the presence of free -NH_2 and −COOH groups. This behavior is also confirmed when the protein is immobilized directly on the TiO_2 surface (TiO_2-BSA sample), showing high wettability with a CA around 17°.

The degree of wetting depends on the relative surface energies of the solids and the liquids on their intermolecular attraction [93]. The surface energy (SE) values had significant variations depending on the molecule present on the surface, as observed in Fig. 5b. SE values increased after the TiO_2 thin film deposition on Ti surface from 39 J/m^2 to 55 J/m^2. This increase can be related to the presence of reactive −OH groups on the surface. The TiO_2-MPA, TiO_2-MPA-BSA, and TiO_2-BSA samples presented increased SE values of 72 J/m^2, 69 J/m^2, and 74 J/m^2, respectively. This higher surface energy can be attributed to the presence of terminal −COOH groups for both samples. In addition, the bio-functionalized surfaces (TiO_2-MPA-BSA and TiO_2-BSA) also presented free -NH_2 groups that can increase the surface energy values. The TiO_2-APTMS did not present significant changes in SE value from

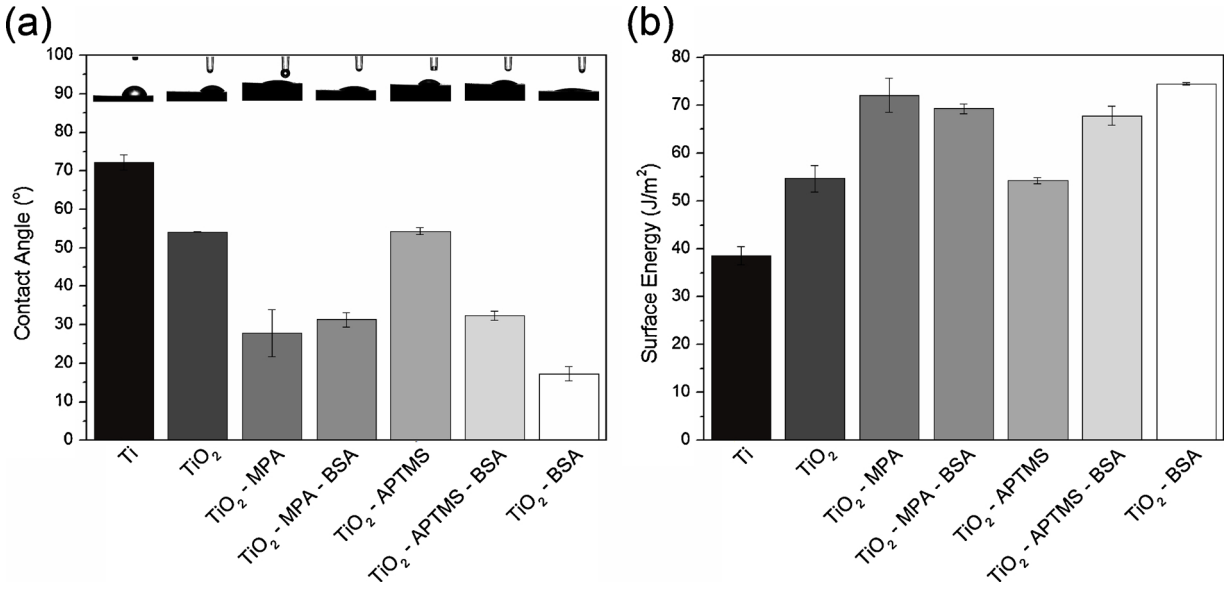

Fig. 5. Water contact angle (a) and surface energy (b) measurements for the functionalized samples.

the TiO_2 sample, showing a SE value of 54 J/m^2. On the other hand, the presence of albumin on TiO_2-APTMS-BSA sample increased the SE value to 68 J/m^2, which may be due to the albumin-free amine (-NH_2) and carboxylic acid (−COOH) groups. For the samples containing albumin, the presence of polar groups on this protein surface increases wettability and surface reactivity by polar liquids [94]. The surface wettability (hydrophilic surface) and surface charge (surface chemistry) of the substrate is an important factor in effective cell interaction with the surfaces, which can affect bone formation, influencing the adhesion, proliferation, and differentiation of osteoblasts [8,95,96]. Tamada et al. [97] determined that surfaces with a contact angle of 70° were suitable for cell adhesion even with surfaces that have poorly controlled roughness and surface load. In general, studies have shown that surfaces with contact angles less than 70° are promising for cell adhesion and proliferation [98].

The different TiO_2 surface modifications under Ti substrates are promising surfaces for cell response, since they have adequate wettability and surface chemistry for adhesion, proliferation, and differentiation of osteoblasts [14,99].

3.4. AFM analysis

To determine the morphological features and roughness of TiO_2, TiO_2-MPA, TiO_2-MPA-BSA, TiO_2-APTMS, TiO_2-APTMS-BSA, and TiO_2-BSA surfaces, AFM measurements were performed, based on a 4.0 μm × 4.0 μm scan of the substrate. The AFM images are presented in Fig. 6.

The TiO_2 substrate had morphology with small spherical domains and low roughness (R_a = 6.25 ± 1.54 nm). TiO_2-MPA and TiO_2-APTMS present different morphology and roughness compared to the TiO_2 substrate, but very similar to each other.

After BSA adsorption on the TiO_2-MPA surface, the morphology and roughness remained similar with a little decrease of Ra, but within the measurement error. For the TiO_2-APTMS substrate, the BSA adsorption maintained the morphology and increased the surface roughness of Ra = 38.90 ± 2.14 nm (TiO_2-APTMS) to Ra = 47.32 ± 2.78 nm (TiO_2-APTMS-BSA).

AFM measurements demonstrate that the BSA adsorption on the TiO_2 substrate increased the roughness to 52.76 ± 1.95 nm, but the morphology was still similar to the surfaces with BSA. In general, a uniform surface, but not homogeneity, was observed with different spherical domains [14,78].

Skewness and Kurtosis parameters were evaluated for the AFM histograms. Skewness is a symmetry measure, or more specifically, the lack of symmetry. Kurtosis is aspect information of a probability distribution. The normal distribution is a symmetrical distribution with well-behaved tails. This is designated by the asymmetry obtained with skewness parameters close to zero and kurtosis values close to 3.00. Obtained values shown a normal distribution of the analyzed histograms, as indicated on caption of Fig. 6.

TiO_2 and functionalized TiO_2 surfaces had different morphologies and roughness. Although the substrates TiO_2-MPA, TiO_2-MPA-BSA, TiO_2-APTMS, TiO_2-APTMS-BSA, and TiO_2-BSA had similar morphologies, the roughness varied among surfaces. Therefore, the variation in morphology, roughness, and contact angle indicates differences in the chemical and wettability of the surface [14,78].

3.5. Cell viability assay

Cell viability of preosteoblast MC3T3-E1 cultured on titanium surfaces and modified substrates (TiO_2, TiO_2-MPA, TiO_2- MPA-BSA, TiO_2-APTMS, TiO_2-APTMS-BSA and TiO_2-BSA) were performed by the MTT reduction assay for 48 and 72 h. MTT assay, the most commonly used method to evaluate the cellular response (viability/cytotoxicity), can measure the increase or decrease of cells that show metabolic activities. Ti substrates were used as the control group [35,100,101].

The results of MTT optical density (OD) values at 550 nm are in Fig. 7.

The results found a gradual increase of cell viability on all surfaces over time. The cell viability at 48 h showed a relative increase for all groups compared with TiO_2, but TiO_2-APTMS presented the highest cell proliferation rate. On the other hand, TiO_2-MPA-BSA, TiO_2-APTMS-BSA, and TiO_2-BSA presented similar viability, although they increased with time. After 72 h, all the substrates presented increased viability, and no statistical difference was found among functionalized surfaces. During the first 48 h, the TiO_2-APTMS substrate had the highest biocompatibility and enhanced cell proliferation rate of MC3T3-E1, even when compared to those with surface immobilized albumin. In general, the functionalized TiO_2 substrates exhibit high biocompatibility and do not introduce toxic materials to the implant surface when compared to the TiO_2 film. As discussed previously, the TiO_2 film is important on the surface of the implant as it decreases the corrosion properties of the material. These biofunctional groups can improve cell adhesion and proliferation properties, as shown by the feasibility results.

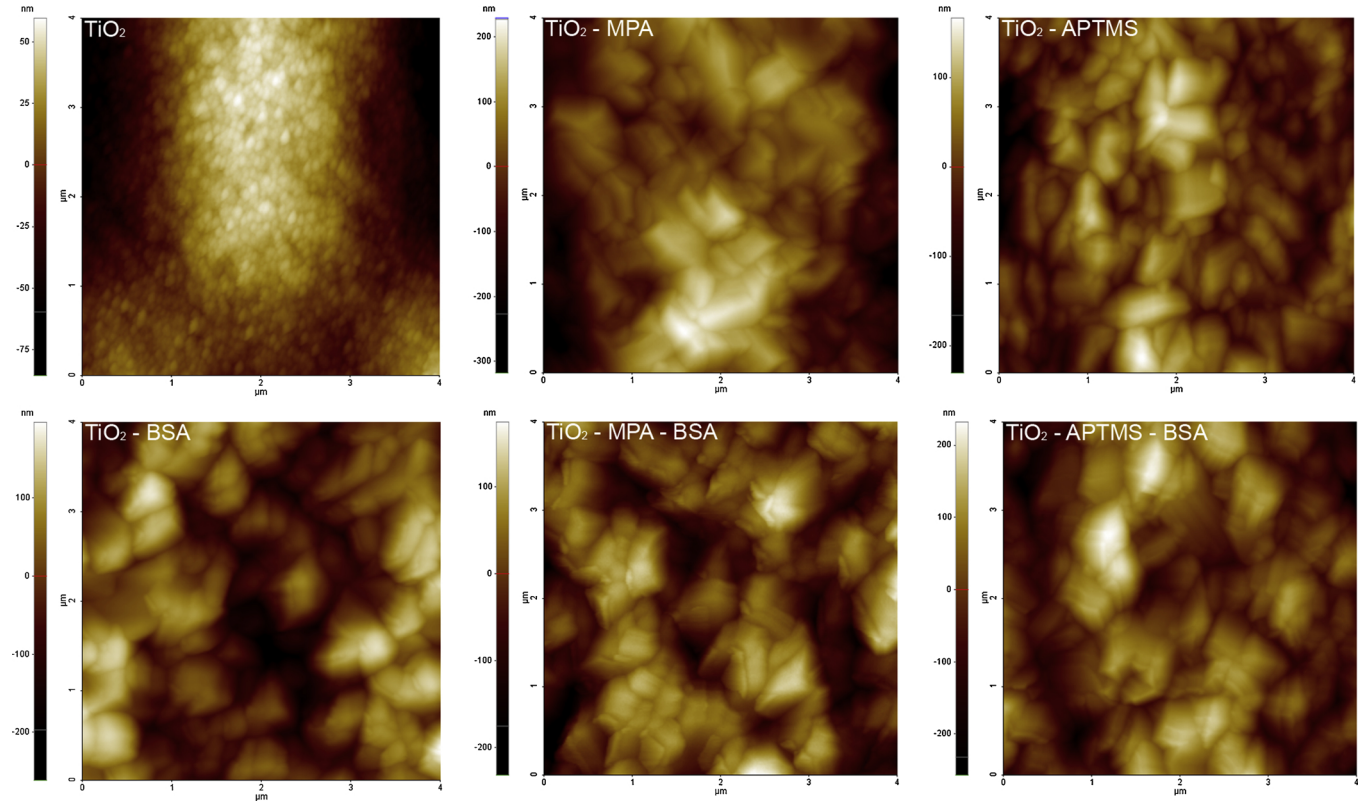

Fig. 6. Two-dimensional AFM images of the surfaces. TiO_2 (6.25 ± 1.54 nm, Rsk = 0.11, Rku = 2.32), TiO_2-MPA (R_a = 41.88 ± 1.93 nm, Rsk = 0.27, Rku = 3.08), TiO_2-APTMS (R_a = 38.90 ± 2.14 nm, Rsk = −0.01, Rku = 2.11) TiO_2-BSA (R_a = 52.76 ± 1.95 nm, Rsk = −0.47, Rku = 2.18), TiO_2-MPA-BSA, (R_a = 37.56 ± 3.42 nm, Rsk = 0.65, Rku = 2.63) and TiO_2-APTMS-BSA (R_a = 47.32 ± 2.78 nm, Rsk = −0.87, Rku = 2.78).

3.6. Alizarin red staining: calcium deposition

To assess the amount of mineral deposited by the cultured cells on the modified surfaces, the calcium deposition in the cell layer was quantified by the alizarin red staining [65,84,102]. The mineralization process was evaluated by determining the Ca^{2+} levels of the supernatants obtained after 14 days of cell culture under the titanium surfaces, through the absorbance measure. Fig. 8 shows the calcium deposition was illustrated by alizarin red on the surfaces at 14 days of culture. As shown in Fig. 8a, calcium deposition is observed as a red color. The mineralization amount was calculated and quantified (Fig. 8b).

On day 14, the cells cultured on the surface-modified Ti surfaces showed a larger amount of calcium. The mineral amount deposited on the different substrates is similar to the deposition found for the titanium substrate, already reported in the literature, as an excellent osteogenic inducer. All modified surfaces had increased extracellular matrix mineralization after 14 days, which indicates that modified TiO_2 surfaces could be a good implant material that helps accelerate the osteogenic differentiation of MC3T3-E1 cells. No statistical difference was found between the different treated surfaces [65, 104, 105].

4. Conclusions

The physical adsorption of albumin on TiO_2 surfaces are not stable and reversible adsorption and desorption processes can occur in the presence of extracellular matrix.

Covalent immobilization of albumin through MPA and APTMS allows better control of albumin on TiO_2 surfaces, with interactions oriented through the groups present on the surface, −COOH when MPA and NH_2 when APTMS, and can optimize cell adhesion and proliferation. However, TiO_2-MPA-BSA and TiO_2-APTMS-BSA exhibited very similar wettability and hydrophilicity, with similar viability and cell mineralization results after 72 h and 14 days, respectively, when

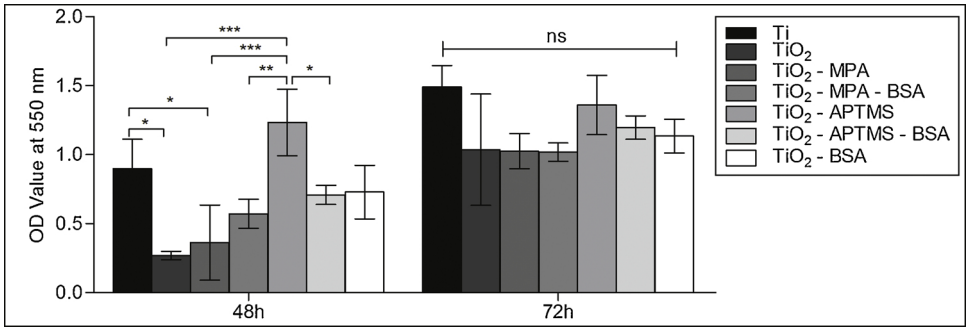

Fig. 7. Cell viability of MC3T3-E1 cells on different surfaces. Metabolic activity of cells surfaces were assessed by MTT assay after 48 and 72 h of culture. (* indicates statistically significant differences ($p < 0.05$)).

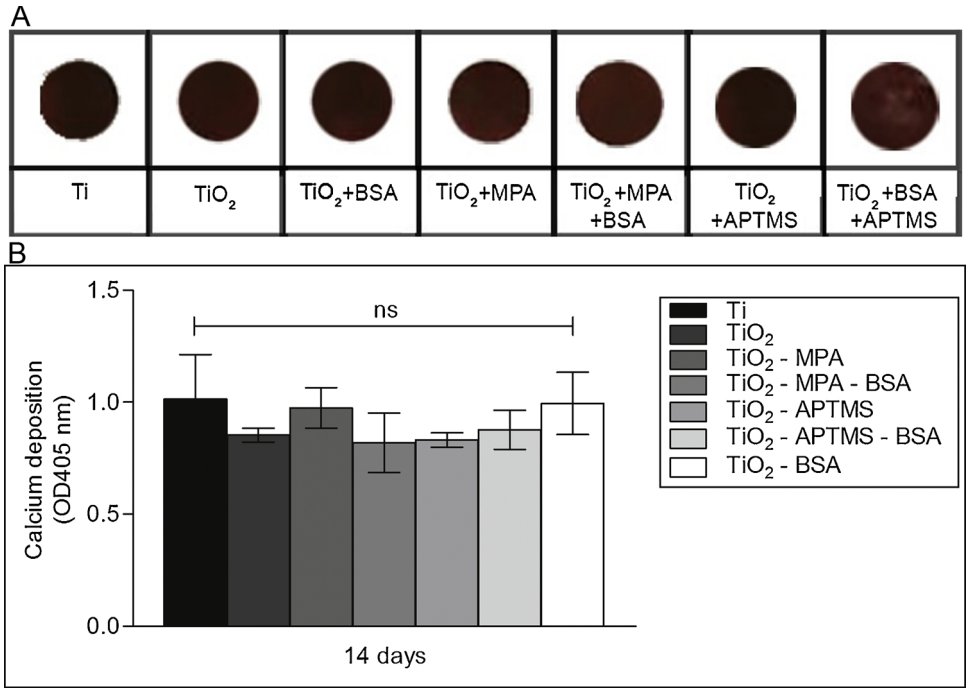

Fig. 8. (a) Images of calcium deposited on Ti modified surfaces, at 14 days of culture and (b) amount of mineralized calcium deposited after 14 days of cultures.

compared to studies of BSA adsorbed directly on TiO_2.

The TiO_2-APTMS substrate had better viability and mineralization results, even with a higher contact angle (54°) than the other substrates analyzed. However, it still had adequate hydrophilicity for cellular interaction. Chemical immobilization of BSA, either physically or covalently, on TiO_2 substrates showed similar surface chemistry without altering long-term cellular interaction. The TiO_2-APTMS substrate with $-NH_2$ groups on the surface is a group that more efficiently interacts with components of the extracellular matrix, presenting high cell viability at 48 h. Therefore, it is possible to conclude that surface chemistry governs the resulting adhesion, proliferation, and differentiation of osteoblastic cells.

Acknowledgment

Authors thank the Brazilian agencies CAPES, CNPq, and FAPESP (2014/01713-3, 2014/20471-0, 2016/11183-7 and 2017/15035-5), for financial support. They are also grateful to Dra Elidiane C. Rangel, UNESO for the contact angle and energy surface measurements and Heloisa Helenna Figueiredo Paes de Oliveira for image design.

References

[1] M. Niinomi, Mechanical properties of biomedical titanium alloys, Mater. Sci. Eng.: A 243 (1998) 231–236.
[2] R. Van Noort, Titanium: the implant material of today, J. Mater. Sci. 22 (1987) 3801–3811.
[3] H.J. Rack, J. Qazi, Titanium alloys for biomedical applications, Mater. Sci. Eng.: C 26 (2006) 1269–1277.
[4] S.J. Lee, M.S. Bae, D.W. Lee, D.N. Heo, D. Lee, M. Heo, S. Hong, J. Kim, W.D. Kim, S.A. Park, I.K. Kwon, The use of heparin chemistry to improve dental osteogenesis associated with implants, Carbohydr. Polym. 157 (2017) 1750–1758.
[5] J.L. Del Pozo, R. Patel, Infection associated with prosthetic joints, N. Eng. J. Med. 361 (2009) 787–795.
[6] J.A. Inzana, Biomaterials approaches to treating implant-associated osteomyelitis, Biomaterials 81 (2016) 58–71.
[7] F. Rupp, R.A. Gittens, L. Scheideler, A. Marmur, B.D. Boyan, Z. Schwartz, J. Geis-Gerstorfer, A review on the wettability of dental implant surfaces I: theoretical and experimental aspects, Acta Biomater. 10 (2014) 2894–2906.
[8] R.A. Gittens, L. Scheideler, F. Rupp, S.L. Hyzy, J. Geis-Gerstorfer, Z. Schwartz, B.D. Boyan, A review on the wettability of dental implant surfaces II: biological and clinical aspects, Acta Biomater. 10 (2014) 2907–2918.
[9] S. Bauer, P. Schmuki, K. von der Mark, J. Park, Engineering biocompatible implant surfaces: part I: materials and surfaces, Prog. Mater Sci. 58 (2013) 261–326.
[10] S.J. Lee, D.N. Heo, J.S. Park, S.K. Kwon, J.H. Lee, J.H. Lee, W.D. Kim, I.K. Kwon, S.A. Park, Characterization and preparation of bio-tubular scaffolds for fabricating artificial vascular grafts by combining electrospinning and a 3D printing system, PCCP 17 (2015) 2996–2999.
[11] X. Liu, P.K. Chu, C. Ding, Surface modification of titanium, titanium alloys, and related materials for biomedical applications, Mater. Sci. Eng.: R: Rep. 47 (2004) 49–121.
[12] R. Tejero, E. Anitua, G. Orive, Toward the biomimetic implant surface, biopolymers on titanium-based implants for bone regeneration, Prog. Polym. Sci. 39 (2014) 1406–1447.
[13] N. Afara, S. Omanovic, M. Asghari-Khiavi, Functionalization of a gold surface with fibronectin (FN) covalently bound to mixed alkanethiol self-assembled monolayers (SAMs): the influence of SAM composition on its physicochemical properties and FN surface secondary structure, Thin Solid Films 522 (2012) 381–389.
[14] E.S. Thian, Z. Ahmad, J. Huang, M.J. Edirisinghe, S.N. Jayasinghe, D.C. Ireland, R.A. Brooks, N. Rushton, W. Bonfield, S.M. Best, The role of surface wettability and surface charge of electrosprayed nanoapatites on the behaviour of osteoblasts, Acta Biomater. 6 (2010) 750–755.
[15] I. Wall, N. Donos, K. Carlqvist, F. Jones, P. Brett, Modified titanium surfaces promote accelerated osteogenic differentiation of mesenchymal stromal cells in vitro, Bone 45 (2009) 17–26.
[16] R.A. Gittens, R. Olivares-Nvarrete, A. Cheng, D.M. Anderson, T. McLachlan, I. Stephan, J. Geis-Gerstorfer, K.H. Sandhage, A.G. Fedorov, F. Rupp, B.D. Boyan, R. Tannenbaum, Z. Schwartz, The roles of titanium surface micro/nanotopography and wettability on the differential response of human osteoblast lineage cells, Acta Biomater. 9 (2013) 6268–6277.
[17] L.D. Trino, L.F.G. Dias, L.G.S. Albano, E.S. Bronze-Uhle, E.C. Rangel, C.F.O. Graeff, P.N. Lisboa-Filho, Zinc oxide surface functionalization and related effects on corrosion resistance of titanium implants, Ceram. Int. 44 (2018) 4000–4008.
[18] F. Rupp, L. Scheideler, N. Olshanska, M. Wild, M. Wieland, J. Geis-Gerstorfer, Enhancing surface free energy and hydrophilicity through chemical modification of microstructured titanium implant surfaces, J. Biomed. Mater. Res. A 76 (2006) 323–334.
[19] F. Rupp, L. Scheideler, D. Rehbein, D. Axmann, J. Geis-Gerstorfer, Roughness induced dynamic changes of wettability of acid etched titanium implant modifications, Biomaterials 25 (2004) 1429–1438.
[20] S.V. Gnedenkov, S.L. Sinebryukhov, V.S. Egorkin, D.V. Mashtalyar, D.A. Alpysbaeva, L.B. Boinovich, Wetting and electrochemical properties of hydrophobic and superhydrophobic coatings on titanium, Colloids Surf. A 383 (2011) 61–66.
[21] A.M. Vilardell, N. Cinca, N. Garcia-Giralt, S. Dosta, I.G. Cano, X. Nogués, J.M. Guilemany, Osteoblastic cell response on high-rough titanium coatings by cold spray, J. Mater. Sci.: Mater. Med. 29 (2018) 1–10.
[22] T. Mekayarajjananonth, S. Winkler, Contact angle measurement on dental implant biomaterials, J. Oral Implantol. 25 (1999) 230–236.
[23] C. Werner, M.F. Maitz, C. Sperling, Current strategies towards hemocompatible coatings, J. Mater. Chem. 17 (2007) 3376–3384.
[24] A. Ochsenbein, F. Chai, S. Winter, M. Traisnel, J. Breme, H.F. Hildebrand, Osteoblast responses to different oxide coatings produced by the sol–gel process on

titanium substrates, Acta Biomater. 4 (2008) 1506–1517.
[25] M.F. Maitz, U. Freudenberg, M.V. Tsurkan, M. Fischer, T. Beyrich, C. Werner, Bio-responsive polymer hydrogels homeostatically regulate blood coagulation, Nat. Commun. 19 (2013) 2168.
[26] Y. Sul, B. Kang, C. Johansson, H. Um, C. Park, T. Albrektsson, The roles of surface chemistry and topography in the strength and rate of osseointegration of titanium implants in bone, J. Biomed. Mater. Res. A 89 (2009) 942–950.
[27] J.S. Shah, P.K.C. Venkatsurya, W.W. Thein-Han, R.D.K. Misra, T.C. Pesacreta, M.C. Somani, L.P. Karjalainen, The role of nanocrystalline titania coating on nanostructured austenitic stainless steel in enhancing osteoblasts functions for regeneration of tissue, Mater. Sci. Eng.: C 31 (2011) 458–471.
[28] S.A. Yavari, J. van der Stok, Y.C. Chai, R. Wauthle, Z. Tahmasebi Birgani, P. Habibovic, M. Mulier, J. Schrooten, H. Weinans, A.A. Zadpoor, Bone regeneration performance of surface-treated porous titanium, Biomaterials 35 (2014) 6172–6181.
[29] R.A. Gittens, R. Olivares-Navarrete, A. Cheng, D.M. Anderson, T. McLachlan, I. Stephan, J. Geis-Gerstorfer, K.H. Sandhage, A.G. Fedorov, F. Rupp, B.D. Boyan, R. Tannenbaum, Z. Schwartz, The roles of titanium surface micro/nanotopography and wettability on the differential response of human osteoblast lineage cells, Acta Biomater. 9 (2013) 6268–6277.
[30] S. Dey, M. Das, V.K. Balla, Effect of hydroxyapatite particle size, morphology and crystallinity on proliferation of colon cancer HCT116 cells, Mater. Sci. Eng., C 39 (2014) 336–339.
[31] Y. Zhukova, C. Hiepen, P. Knaus, M. Osterland, S. Prohaska, J.W.C. Dunlop, P. Fratzl, E.V. Skorb, The role of titanium surface nanostructuring on preosteoblast morphology, adhesion, and migration, Adv. Healthcare Mater. 6 (2017) 1601244.
[32] L. Le Guéhenne, A. Soueidan, P. Layrolle, Y. Amouriq, Surface treatments of titanium dental implants for rapid osseointegration, Dent. Mater. 23 (2007) 844–854.
[33] S.P. Pilipchuk, A.B. Plonka, A. Monje, A.D. Taut, A. Lanis, B. Kang, W.V. Giannobile, Tissue engineering for bone regeneration and osseointegration in the oral cavity, Dent. Mater. 31 (2015) 317–338.
[34] T. Hanawa, A comprehensive review of techniques for biofunctionalization of titanium, J. Periodont. Implant Sci. 41 (2011) 263–272.
[35] Y. Xiaohua, J. Walshb, M. Wei, Covalent immobilization of collagen on titanium through polydopamine coating to improve cellular performances of MC3T3-E1 cells, RSC Adv. 4 (2014) 7185–7192.
[36] D.B.S. Mendonça, P.A. Miguez, G. Mendonça, M. Yamauchi, F.J.L. Aragão, L.F. Cooper, Titanium surface topography affects collagen biosynthesis of adherent cells, Bone 49 (2011) 463–472.
[37] D.G. Castner, B.D. Ratner, Biomedical surface science: foundations to frontiers, Surf. Sci. 500 (2002) 28–60.
[38] M. Tirrell, E. Kokkoli, M. Biesalski, The role of surface science in bioengineered materials, Surf. Sci. 500 (2002) 61–83.
[39] A. Bhogale, N. Patel, P. Sarpotdar, J. Mariam, P.M. Dongre, A. Miotello, D.C. Kothari, Systematic investigation on the interaction of bovine serum albumin with ZnO nanoparticles using fluorescence spectroscopy, colloids surf, B: Biointerfaces 102 (2013) 257–264.
[40] D.R. Schmidt, H. Waldeck, W.J. Kao, D.A. Puleo, R. Bizios (Eds.), Biol. Interact. Mater. Surf. Springer, US, 2009, pp. 1–18.
[41] P. Silva-Bermudez, S.E. Rodil, An overview of protein adsorption on metal oxide coatings for biomedical implants, Surf. Coat. Technol. 233 (2013) 147–158.
[42] J.D. Andrade, V. Hlady, Biopolym.-Exclusion HPLC, Springer Berlin Heidelberg, 1986, pp. pp. 1–63.
[43] L. Vroman, A.L. Adams, G.C. Fischer, P.C. Munoz, Interaction of high molecular weight kininogen, factor XII, and fibrinogen in plasma at interfaces, Blood 55 (1980) 156–159.
[44] S. Dumon, H. Barnier, Ultrafiltration of protein solutions on ZrO2 membranes. The influence of surface chemistry and solution chemistry on adsorption, J. Membr. Sci. 74 (1992) 289–302.
[45] Z.Y. Huang, M. Chen, S.R. Pan, D.H. Chen, Effect of surface microstructure and wettability on plasma protein adsorption to ZnO thin films prepared at different RF powers, Biomed. Mater. 5 (2010) 054116.
[46] T. Kopac, K. Bozgeyik, Effect of surface area enhancement on the adsorption of bovine serum albumin onto titanium dioxide, colloids surf, B: Biointerfaces 76 (2010) 265–271.
[47] L. Song, K. Yang, W. Jiang, P. Du, B. Xing, Adsorption of bovine serum albumin on nano and bulk oxide particles in deionized water, colloids surf, B Biointerfaces 94 (2012) 341–346.
[48] B. Groessnerschreiber, R.S. Tuan, Enhanced extracellular-matrix production and mineralization by osteoblasts cultured on titanium surfaces in vitro, J. Cell Sci. 101 (1992) 209–217.
[49] T. Sjöström, A.S. Brydone, R.M.D. Meek, M.J. Dalby, B. Su, L.E. McNamara, Titanium nanofeaturing for enhanced bioactivity of implanted orthopedic and dental devices, Nanomedicine 8 (2013) 89–104.
[50] M.S. Killian, Organic Modification of TiO_2 and Other Metal Oxides With SAMs and Proteins - a Surface Analytical Investigation, PhD thesis School of Engineering, Friedrich-Alexander-Universität Erlangen-Nürnberg, Nürnberg, 2013 pp. 233.
[51] H. Wang, D.G. Castner, B.D. Ratner, S.Y. Jiang, Probing the orientation of surface-immobilized immunoglobulin G by time-of-flight secondary ion mass spectrometry, Langmuir 20 (2004) 1877–1887.
[52] Q.J. Chi, J.D. Zhang, J.E.T. Andersen, J. Ulstrup, Ordered assembly and controlled electron transfer of the Blue copper protein Azurin at Gold (111) single-crystal substrates, J. Phys. Chem. B 105 (2001) 4669–4679.
[53] S.F. Chen, L.Y. Liu, J. Zhou, S.Y. Jiang, Controlling antibody orientation on charged self-assembled monolayers, Langmuir 19 (2003) 2859–2864.
[54] J.G. Fraaije, J.M. Kleijn, M. Vandergraaf, J.C. Dijt, Orientation of adsorbed cytochrome c as a function of the electrical potential of the interface studied by total internal reflection fluorescence, Biophys. J. 57 (1990) 965–975.
[55] M.A. Bos, J.M. Kleijn, Determination of the orientation distribution of adsorbed fluorophores using TIRF. II. Measurements on porphyrin and cytochrome c, Biophys. J. 68 (1995) 2573–2579.
[56] J.E. Lee, S.S. Saavedra, Molecular orientation in heme protein films adsorbed to hydrophilic and hydrophobic glass surfaces, Langmuir 12 (1996) 4025–4032.
[57] N. Adden, L.J. Gamble, D.G. Castner, A. Hoffmann, G. Gross, H. Menzel, Phosphonic acid monolayers for binding of bioactive molecules to titanium surfaces, Langmuir 22 (2006) 8197–8204.
[58] C.A. Middleton, C.J. Pendegrass, D. Gordon, J. Jacob, G.W. Blunn, Fibronectin silanized titanium alloy: a bioinductive and durable coating to enhance fibroblast attachment in vitro, J. Biomed. Mater. Res. 83 (2007) 1032–1038.
[59] S.P. Pujari, L. Scheres, A.T.M. Marcelis, H. Zuilhof, Covalent surface modification of oxide surfaces, Angew. Chem. Int. Ed. 53 (2014) 6322–6356.
[60] J.C. Love, L.A. Estroff, J.K. Kriebel, R.G. Nuzzo, G. M. whitesides. Self-assembled monolayers of thiolates on metals as a form of nanotechnology, Chem. Rev. 105 (2005) 1103–1169.
[61] N. Metoki, L. Liu, E. Beilis, N. Eliaz, D. Mandler, Preparation and characterization of alkylphosphonic acid self assembled monolayers on titanium alloy by chemisorption and electrochemical deposition, Langmuir 30 (2014) 6791–6799.
[62] E.S. Gawalt, M.J. Avaltron, M.P. Danahy, B.M. Silverman, E.L. Hanson, K.S. Midwood, J.E. Schwarzbauer, J. Schwartz, Bonding organics to Ti alloys: facilitating human osteoblast attachment and spreading on surgical implant materials, Langmuir 19 (2003) 200–204.
[63] S. Bozzini, P. Petrini, M.C. Tanzi, S. Zürcher, S. Tosatti, Poly(ethylene glycol) and hydroxy functionalized alkane phosphate mixed self-assembled monolayers to control nonspecific adsorption of proteins on titanium oxide surfaces, Langmuir 26 (2010) 6529–6534.
[64] E. Kim, T. Kim, J. Jung, S.O. Hong, D. Lee, Enhanced osteogenic differentiation of MC3T3-E1 on rhBMP-2-immobilized titanium via click reaction, Carbohydr. Polym. 103 (2014) 170–178.
[65] L. Li1, S. Kim, S. Cho1, Comparison of alkaline phosphatase activity of MC3T3-E1 cells cultured on different Ti surfaces: modified sandblasted with large grit and acid-etched (MSLA), laser-treated, and laser and acid-treated Ti surfaces, J. Adv. Prosthodont. 8 (2016) 235–240.
[66] C.C. Wachesk, C.A.F. Pires, B.C. Ramos, V.J. Trava-Airoldi, A.O. Lobo, C. Pacheco-Soares, F.R. Marciano, N.S. Da-Silva, Cell viability and adhesion on diamond-like carbon films containing titanium dioxide nanoparticles, Appl. Surf. Sci. 266 (2013) 176–181.
[67] L.T. Allen, M. Tosetto, I.S. Miller, D.P. O'Connor, S.C. Penney, I. Lynchb, A.K. Keenan, S.R. Pennington, K.A. Dawson, W.M. Gallagher, Surface-induced changes in protein adsorption and implications for cellular phenotypic responses to surface interaction, Biomaterials 27 (2006) 3096–3108.
[68] M. Pegueroles, C. Tonda-Turo, J.A. Planell, F. Gil, C. Aparicio, Adsorption of fibronectin, fibrinogen, and albumin on TiO_2: time-resolved kinetics, structural changes, and competition study, Biointerfaces 7 (2012) 1–4.
[69] M.A. McArthur, T.M. Byrne, R.J. Sanderson, G.P. Rockwell, L.B. Lohstreter, Bai Z, M.J. Filiaggi, J.R. Dahn, An in situ study of protein adsorption on combinatorial Cu–Al films using spectroscopic ellipsometry, Colloids Surf., B 81 (2010) 58–66.
[70] Y. Arima, H. Iwata, Preferential adsorption of cell adhesive proteins from complex media on self-assembled monolayers and its effect on subsequent cell adhesion, Acta Biomater. 26 (2015) 72–81.
[71] K. Chen, W.B. Caldwell, C.A. Mirkin, Fullerene self-assembly onto (MeO)3Si(CH2)3NH2-modified oxide surfaces, J. Am. Chem. Soc. 115 (1993) 1193–1194.
[72] U. Jonsson, M. Malmqvist, G. Olofsson, I. Ronnberg, Surface immobilization techniques in combination with ellipsometry, Methods Enzymol. 137 (1988) 381–388.
[73] J. Chen, J. Cao, J. Wang, M.F. Maitz, L. Guo, Y. Zhao, Q. Li, K. Xiong, N. Huang, Biofunctionalization of titanium with PEG and anti-CD34 for hemocompatibility and stimulated endothelialization, J. Colloid Interface Sci. 368 (2012) 636–647.
[74] L.D. Trino, E.S. Bronze-Uhle, A. George, M.T. Mathew, P.N. Lisboa-Filho, Surface physicochemical and structural analysis of functionalized titanium dioxide films, Colloids Surf., A 546 (2018) 168–178.
[75] M. Lewandowska, A. Rogusk, M. Pisarek, B. Polak, M. Janik-Czachor, K.J. Kurzydłowski, Morphology and chemical characterization of Ti surfaces modified for biomedical application, Biomol. Eng 24 (2007) 438–444.
[76] M.C. Martins, B.D. Ratner, M.A. Barbosa, Protein adsorption on mixtures of hydroxyl- and methylterminated alkanethiols self-assembled monolayers, J. Biomed. Mater. Res. Part A 67 (2003) 158–171.
[77] E.M.E. Kristensen, F. Nederberg, H. Rensmo, T. Bowden, J. Hilborn, S. Siegbahn, Photoelectron spectroscopy studies of the functionalization of a silicon surface with a phosphorylcholine-terminated polymer grafted onto (3-aminopropyl) trimethoxysilane, Langmuir 22 (2006) 9651–9657.
[78] M. Advincula, X. Fan, J. Lemons, R. Advincula, Surface modification of surface sol–gel derived titanium oxide films by self-assembled monolayers (SAMs) and non-specific protein adsorption studies, Colloids Surf., B 42 (2005) 29–43.
[79] J.F. Moulder, Handbook of X-ray photoelectron spectroscopy: a reference book of standard spectra for identification and interpretation of XPS data; Physical electronics division, Perkin-Elmer Corporation (1992).
[80] F.K. Hansen, G. Rødsrud, Surface tension by pendant drop: I. A fast-standard instrument using computer image analysis, J. Colloid Interface Sci. 141 (1991) 1–9.
[81] K. Subramani1, S.N. Pandruvadal, D.A. Puleo, J.K. Hartsfield Jr, S.S. Huja1, In vitro evaluation of osteoblast responses to carbon nanotube-coated titanium surfaces, Progress in Orthodontics 17 (2016).

[82] F.A. Oliveira, A.A. Matos, S.S. Matsuda, M.A. Buzalaf, V.S. Bagnato, M.A. Machado, et al., Low level laser therapy modulates viability, alkaline phosphatase and matrix metalloproteinase-2 activities of osteoblasts, J. Photochem. Photobiol. B. 28 (2017) 35–40.
[83] T. Mosmann, Rapid colorimetric assay for cellular growth and survival:application to proliferation and cytotoxicity assays, J. Immunol. Methods 65 (1983) 55–63.
[84] F.A. Oliveira, A.A. Matos, M.R. Santesso, C.K. Tokuhara, A.L. Leite, V.S. Bagnato, et al., Low intensity lasers differently induce primary human osteoblast proliferation and differentiation, J. Photochem. Photobiol. B. 163 (2016) 14–21.
[85] D.G. Castner, K. Hinds, D.W. Grainger, X-ray photoelectron spectroscopy sulfur 2p study of organic thiol and disulfide binding interactions with Gold surfaces, Langmuir 12 (1996) 5083–5086.
[86] G. Gonella, O. Cavalleri, S. Terreni, D. Cvetko, L. Floreano, A. Morgante, M. Canepa, R. Rolandi, High resolution X-ray photoelectron spectroscopy of 3-mercaptopropionic acid self-assembled films, Surf. Sci. 566–568 (2004) 638–643.
[87] Y.L. Khung, S.H. Ngalim, A. Scaccabarozi, D. Narducci, Thermal and UV hydrosilylation of alcohol-based bifunctional alkynes on Si (111) surfaces: how surface radicals influence surface bond formation, Sci. Rep. 5 (2015) 11299.
[88] E. Ataman, C. Isvoranu, J. Knudsen, K. Schulte, J.N. Andersen, J. Schnadt, Adsorption of L-cysteine on rutile TiO2(110), Surf. Sci. 605 (2011) 179–186.
[89] Y.Y. Song, H. Hildebrand, P. Schmuki, Optimized monolayer grafting of 3-aminopropyltriethoxysilane onto amorphous, anatase and rutile TiO_2, Surf. Sci. 604 (2010) 346–353.
[90] O.P. Kharbanda, J. Sharan, V. Koul, A.K. Dinda, M. Mishra, G. Gupta, M.P. Singh, Tethering of 3-aminopropyltriethoxy silane films on medical grade v titanium alloy surface through self-assembled monolayers (SAMs) for biomedical applications, Appl. Surf. Sci. 412 (2017) 648–656.
[91] M.H. Ahmed, T.E. Keyes, J.A. Byrne, C.W. Blackledge, J.W. Hamilton, Adsorption and photocatalytic degradation of human serum albumin on TiO2 and Ag–TiO2 films, J. Photochem. Photobiol., A 222 (2011) 123–131.
[92] S.R. Sousa, P. Moradas-Ferreira, B. Saramago, L.V. Melo, M.A. Barbosa, Human serum albumin adsorption on TiO2 from single protein solutions and from plasma, Langmuir 20 (2004) 9745–9754.
[93] J.M. Powers, J.C. Wataha, Dental Materials: Properties and Manipulation, 9th ed., Elsevier, Missouri, 2011.
[94] T. Bialopiotrowicz, B. Jańczuk, Wettability and surface free energy of bovine serum albumin films, J. Surfactants Deterg. 4 (2001) 287–292.
[95] S.J. Lee, D.N. Heo, H.R. Lee, D. Lee, S.J. Yu, S.A. Park, W. Ko, S.W. Park, S.G. Im, J. Moon, I.K. Kwon, Biofunctionalized titanium with anti-fouling resistance by grafting thermo-responsive polymer brushes for the prevention of peri-implantitis, J. Mater. Chem. B 26 (2015) 5161–5165.
[96] Y. Arima, H. Iwata, Effect of wettability and surface functional groups on protein adsorption and cell adhesion using well-defined mixed self-assembled monolayers, Biomaterials 28 (2007) 3074–3082.
[97] Y. Tamada, Y. Ikada, Effect of preadsorbed proteins on cell adhesion to polymer surfaces, J. Colloid. Interface Sci. 155 (1993) 334–339.
[98] J.H. Lee, G. Khang, J.W. Lee, H.B. Lee, Interaction of different types of cells on polymer surfaces with wettability gradient, J. Colloid. Interface Sci. 205 (1998) 323–330.
[99] D.H. Yang, S.W. Moon, D. Lee, Surface modification of titanium with BMP-2/GDF-5 by a heparin linker and its efficacy as a dental implant, Int. J. Mol. Sci. 18 (2017) 229–245.
[100] W. Wang, T.L. Li, H.M. Wong, P.K. Chu, R.Y.T. Kao, S. Wu, F.K.L. Leung, T.M. Wong, M.K.T. To, K.M.C. Cheung, K.W.K. Yeung, Development of novel implants with self-antibacterial performance through in-situ growth of 1D ZnO nanowire, Colloids Surf., B 141 (2016) 623–633.
[101] Antibacterial efficacy, Corrosion resistance, and cytotoxicity studies of copper-substituted carbonated hydroxyapatite coating on titanium substrate, J. Mater Sci. 50 (2015) 1688–1700.
[102] S.J. Lee, D. Lee, T.R. Yoon, H.K. Kim, H.H. Jo, J.S. Park, J.H. Lee, W.D. Kim, I.K. Kwon, S.A. Park, Surface modification of 3D-printed porous scaffolds via mussel-inspired polydopamine and effective immobilization of rhBMP-2 to promote osteogenic differentiation for bone tissue engineering, Acta Biomater. 40 (2016) 182–191.